Integration of parallel pathways for flight control in a hawkmoth reflects prevalence and relevance of natural visual cues

Ronja Bigge[1,2], Rebecca Grittner[1], Anna Stöckl*[1,2]

[1] *Behavioral Physiology and Sociobiology (Zoology II), University of Würzburg, Biozentrum am Hubland, 97074 Würzburg, Germany*

[2] *Department of Biology, University of Konstanz, Universitätsstr. 10, 78464 Konstanz, Germany*

* corresponding author: Anna Stöckl, anna.stoeckl@uni-konstanz.de

Abstract

An animal's behaviour is the result of multiple neural pathways acting in parallel, receiving information across and within sensory modalities at the same time. How these pathways are integrated, particularly when their individual outputs are in conflict, is key to understanding complex natural behaviours. We investigated this question in the visually guided flight of the hummingbird hawkmoth *Macroglossum stellatarum*. These insects were recently shown to partition their visual field, using ventrolateral optic-flow cues to guide their flight like most insects, while the same stimuli in the dorsal visual field evoke a novel directional response. Using behavioural experiments which set the two pathways into conflict, we tested whether and how the ventrolateral and dorsal pathway integrate to guide hawkmoth flight. Combined with environmental imaging we demonstrate that the partitioning of the visual field followed the prevalence of visual cues in the hawkmoths' natural habitats, while the integration hierarchy of the two pathways matched the relevance of these cues for the animals' flight safety, rather than their magnitude in the experimental setup or in natural habitats. These results provide new mechanistic insights into the vision-based flight control of insects, and link these to their natural context. We anticipate our findings to be the starting point for comparative investigations into parallel pathways for flight guidance in insects from differently structured natural habitats.

Keywords

vision, natural scenes, parallel processing, flight control, optic flow, orientation

Introduction

An animals' behaviour is rarely guided just by one neural pathway or sensory modality. More often, parallel input from multiple sensory modalities supports various control systems at any given time: an insect might be following an odour plume, for example, while guiding its flight safely using visual and mechanosensory cues [1, 2]. Even within the same modality, multiple pathways might act in parallel to shape the same behavioural output [3-5]. How these parallel pathways are integrated, particularly when their individual outputs are in conflict, is key to understanding the complex natural behaviour of animals [6]. This question can be particularly well investigated in a context where the same visual stimuli evoke different responses in different parts of the visual field. Such visual field partitioning is widespread among animals, and likely shaped by the frequency at which these stimuli occur in the natural habitats of the animals [7-9].

We recently described a unique example of functional visual field partitioning in a hawkmoth: the hummingbird hawkmoth *Macroglossum stellatarum* uses translational optic-flow, the perceived relative motion of the environment generated by the animals' own motion [10], only in their ventral and lateral visual field for flight guidance, while the same stimuli in the dorsal visual field evoke a directional response [11] (Fig. 1A). In this directional response, they orient their flight along the main axis of different types of patterns, which is reminiscent of the dorsal orientation responses of ants under tree canopies [12]. This behavioural partitioning matches the reliability of occurrence of translational optic flow and contrast cues across the different regions of the visual field [11, 13, 14] (Fig. 1B).

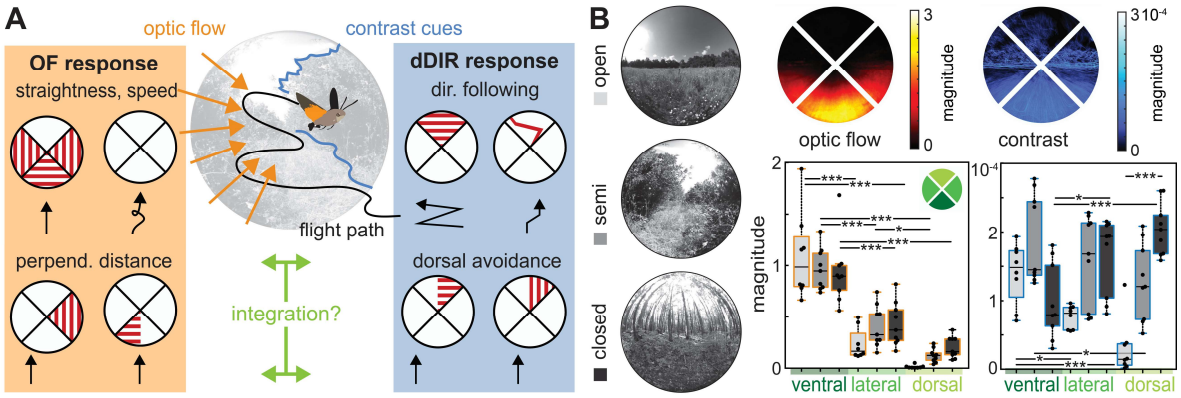

Fig. 1 Optic flow and directional responses partition the visual field for flight control in the hummingbird hawkmoth. A Flight control in most insects is strongly based on optic flow, the apparent movement of the environment across the visual field, induced by the animals' own movement. Ventrolateral translational optic flow supports straight flight, compared to featureless environments. Most insects keep the magnitude of translational optic flow constant across their eyes, by adjusting their speed and perpendicular distance to optic-flow inducing textures. In hawkmoths, optic-flow cues presented in the dorsal visual field induce directional responses, which align the hawkmoths' flight with the main direction of the visual cue. Moreover, hawkmoths avoid any structures in the dorsal, but not the ventral, visual field, even if they generate only weak translational optic flow. **B** The distribution of optic flow and contrast cues was measured across different habitat types: open (no bushes or trees within 500m of the camera), semi-open (lateral vegetation but no closed canopy) and closed (entirely closed canopy). The left column shows an example image of each habitat type. Boxplots depict the mean magnitude of translational optic flow (left panel) and contrast edges (right panel) across habitat types, and for three different scenes within habitats in the dorsal, ventral and lateral segments of the visual field (see coloured inset). Statistical results from a linear mixed-effects model are abbreviated as * $p < 0.05$, ** $p < 0.01$, *** $p < 0.001$.

Typically, insect flight control is known to strongly rely on translational optic flow, to regulate particularly flight speed [15-20] and the distance to the surrounding environment [15, 16, 21-26]. Comparable responses were found for hummingbird hawkmoths [27, 28]. This regulation is likely achieved by keeping the perceived rate of translational optic flow at a constant level across both eyes and over time [19, 29]. In consequence, when insects encounter features that change contrast in the direction of travel, and thus generate translational optic flow, such as an array of trees or a vertically patterned wall in a flight tunnel, they slow down and keep a greater distance. Thereby, they reduce the perceived magnitude of translational optic flow. Optic flow cues are also used to guide flight straightness, particularly when presented in the ventral visual field [11, 30]. It is thought that insects measure optic flow across their entire visual field, and respond to the area with the highest magnitude of translational optic flow within [19, 31]. While this assumption has rarely been tested with dorsal optic flow cues, in honeybees and fruit flies, dorsal optic flow responses similar to the ventrolateral ones have been described [19, 32]. Thus, hawkmoths are currently the only insect species for which a partitioning of the visual field has been demonstrated in terms of optic-flow-based flight control [33-35].

We therefore characterised the unique directional response of the hummingbird hawkmoths, to test its similarity to translational optic-flow based flight responses. To this aim, we performed behavioural investigations of hummingbird hawkmoths in flight tunnels. Unlike other examples of visual field partitioning, such as landing and predator avoidance to looming stimuli in fruit flies [36], the hawkmoth flight responses to dorsal and ventrolateral visual cues are not functionally exclusive, suggesting these processes might act in parallel. To dissect the integration hierarchies of the dorsal response and ventrolateral optic-flow-based flight control, we applied cue conflict experiments, such as commonly used in multisensory integration studies [37, 38]. We evaluated the magnitude of optic flow and contrast cues in different parts of the visual field in our experimental setups, and set these into context with natural visual scenes, to understand the ecological relevance of the integration hierarchies of the parallel pathways for flight guidance in the hummingbird hawkmoth.

Results

We monitored the hawkmoths' behaviour in flight tunnels, which they traversed on their way between two cages with hidden feeders (Fig. 2A). From the tracked and digitized flight paths (Fig. 2B), we extracted features of their flight responses: the average frame-by-frame flight speed, the position relative to the midline, the relative proportion of movement along the long versus short axis of the tunnel, and the cross-index (difference in lateral position at the exit versus entrance, Fig. 2C). When translational optic flow (henceforth called optic flow) was presented laterally, hawkmoths kept a perpendicular distance to the respective walls, resulting in either shifts in the median position relative to the midline when only one wall generated optic flow (Fig. 2D), or a centring of flight paths around the midline with symmetric distances when both walls did (Fig. 2D). We indirectly measured the relative vertical position of the hawkmoths in the tunnels, and thereby their distance to dorsal and ventral patterns, by the size of the moths' image in the videos (see Methods). While this indirect measure must be treated with caution, the general trends are indicative of optic flow responses: hawkmoths flew higher, and thus further away from ventral optic flow patterns compared to flights without patterns (Fig. S1D). This was also the case when the optic flow patterns only extended over one side of the ventral tunnel (Fig. S1H). Moreover, hawkmoths flew at a similar height with longitudinal ventral gratings (which generated little optic flow) as without patterns, and significantly lower than with perpendicular ventral gratings (Fig. S3C). Thus, both for lateral and ventral cues, hawkmoths kept a greater perpendicular distance from high - compared to low optic flow patterns.

Previous work has shown that the distance hawkmoths keep to lateral optic flow depends on its spatial resolution and contrast, and is largest for the optimal resolution and highest contrast, while the effect of lateral optic flow on flight speed and flight straightness remained similar for all patterns that hawkmoths could perceive [11, 39]. With the limited range of spatial frequencies tested for ventral patterns, we did not observe a significant difference in vertical distance for different spatial frequencies. This might have been due to differences in the pattern structure (previous studies used sinewave and checkerboards rather than square-wave gratings), or the very coarse measure of distance applied here. Like with lateral optic flow patterns (Fig. 2E,F), ventral optic flow patterns induced a reduction in lateral movement (Fig. S1C), and flight speed (Fig. S1F).

Directional responses were characterised by a much stronger reduction in flight speed than observed for lateral or ventral optic flow cues (Fig. 2E), and highly increased lateral movement (Fig. 2F). This increased lateral movement was caused by an alignment of the hawkmoths' flight direction with the main axis of the dorsal cue. It was most clearly observable with a stimulus that crossed from one side of the tunnel to the other, which resulted in an according change in the hawkmoths' lateral position across the tunnel (Fig. 2G). Such a switch in lateral position was never observed with ventral stimuli (Fig. 2G). Moreover, with dorsal gratings of different spatial frequencies, hawkmoths showed a proportional change in lateral movement, consistent with following the stripes' directional information, more so for higher spatial frequencies (Fig. 2I). For ventral gratings, the proportion of lateral movement and flight speed did not show a consistent variation with stripe frequency (Fig. S1C).

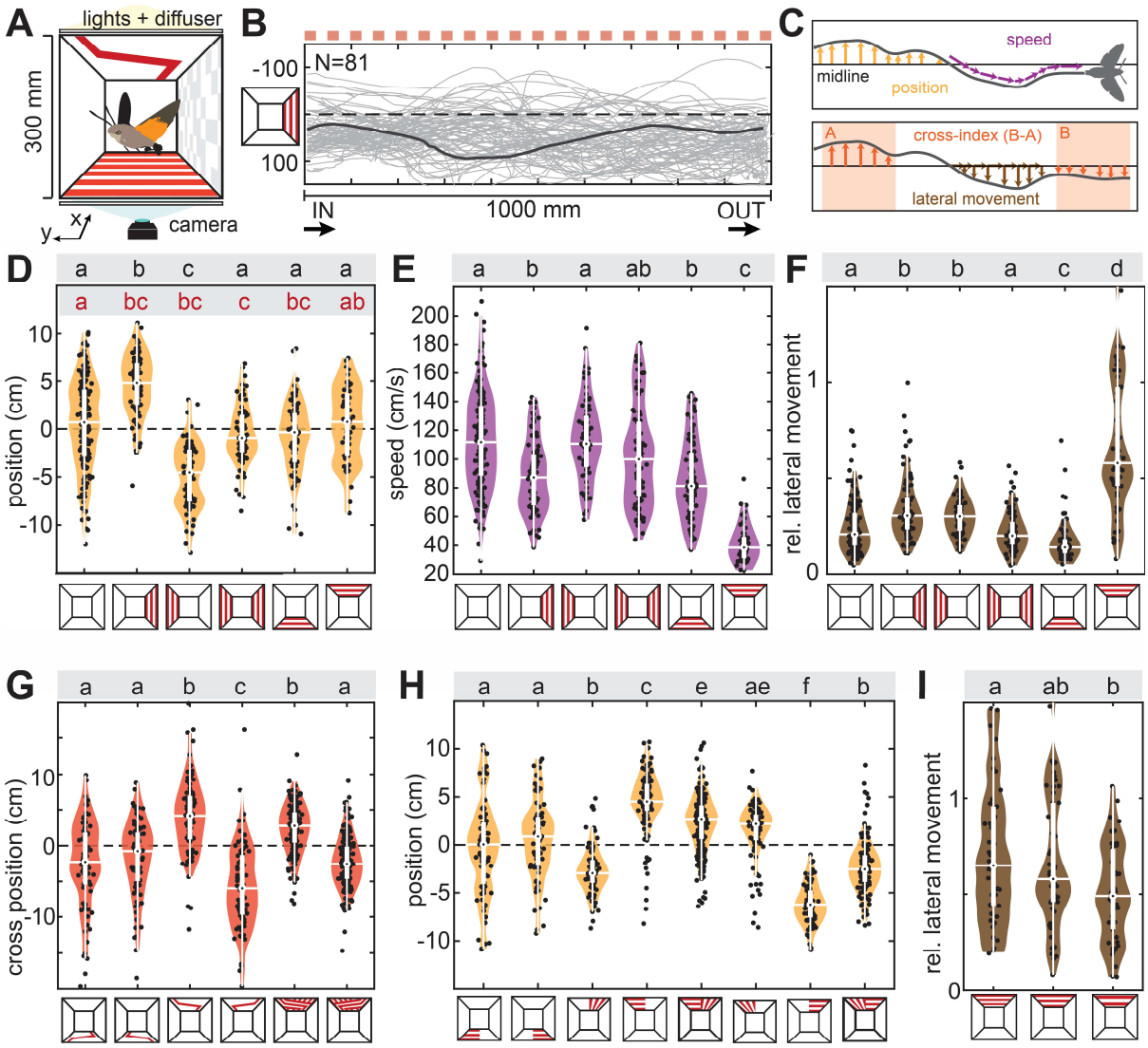

Fig. 2 **Optic-flow-based flight control and dorsal directional responses.**
A Hawkmoth flight behaviour was tested in a 100 cm long, 30-by-30 cm diameter tunnel, which could present visual patterns on any face to generate translational optic flow and directional cues. **B** The hawkmoths' flight paths (shown from the camera's perspective) were digitized with a camera mounted below the tunnel. N gives the number of flights. The dark grey line highlights one representative path. **C** From the flight paths, we quantified the median position off the midline, the average frame-by-frame speed, the proportion of lateral movement (as the ratio of frame-by-frame movement perpendicular and parallel to the longitudinal axis of the tunnel), and the cross-index; the difference in lateral position in the first and last third of the tunnel. **D-F** Median position, average speed and proportion of lateral movement with grating patterns on either tunnel side. **G** Cross-index with a red stripe which changed its position in the central third of the tunnel, crossing from one tunnel side to the other. The last two conditions present a version of this stripe, which repeated at the same spatial frequency as the grating patterns. **H** Median position of flight tracks with gratings perpendicular (generating strong translational optic flow) and parallel (weak translational optic flow) to the tunnel's longitudinal axis, covering one side of either the tunnel ceiling or floor. **I** Proportion of lateral movement with gratings of different spatial frequencies (repeating every 3 cm, 6 cm and 12 cm), mounted to the tunnel ceiling. Black letters in **D-I** show statistically significant differences in group medians (confidence level: 5%). The red letters in **D** represent statistically significant differences in group variance from pairwise Brown–Forsythe tests (significance level 5%). The white boxplots depict the median and 25% to 75% range, the whiskers represent the data exceeding the box by more than 1.5 interquartile ranges, and the violin plots indicate the distribution of the individual data points shown in black.

Together with increasing lateral movement, hawkmoths reduced their flight speed moderately even for a single dorsal line stimulus, which covered only a small portion of the dorsal visual field (Fig. S2A), and drastically for all dorsal contrast patterns that covered at least half the tunnel ceiling, even if they did not generate strong optic flow cues (Fig. S2A,B,I). If possible, hawkmoths strictly avoided flying under dorsal coverage of the tunnel, the more so, the stronger it contrasted against the flight direction (Fig. 2H). On the other hand, hawkmoths did neither avoid nor seek out flying over contrasting structures in the ventral visual field (Fig. 2H). Interestingly, unlike for lateral and ventral gratings, hawkmoths did not keep a greater perpendicular distance to dorsal gratings (Fig. S1D, G, S3C). On the contrary, they flew closer to the tunnel ceiling in these conditions than in tunnels without patterns, and mostly at a similar height than with ventral patterns. In tunnels with dorsal gratings covering one side, in which the moths flew exclusively on the free side, they remained at a similar height than in tunnels without patterns (Fig. S1H).

Taken together, these observations suggest that the hummingbird hawkmoths' directional responses to contrast patterns in the dorsal visual field did not bear hallmarks of optic-flow-based flight response, as in the ventrolateral visual field. This strongly suggests that a different visual pathway underlies this flight behaviour. We therefore asked next, whether the responses to dorsal versus ventrolateral stimuli resulted from independent control systems, which act in parallel.

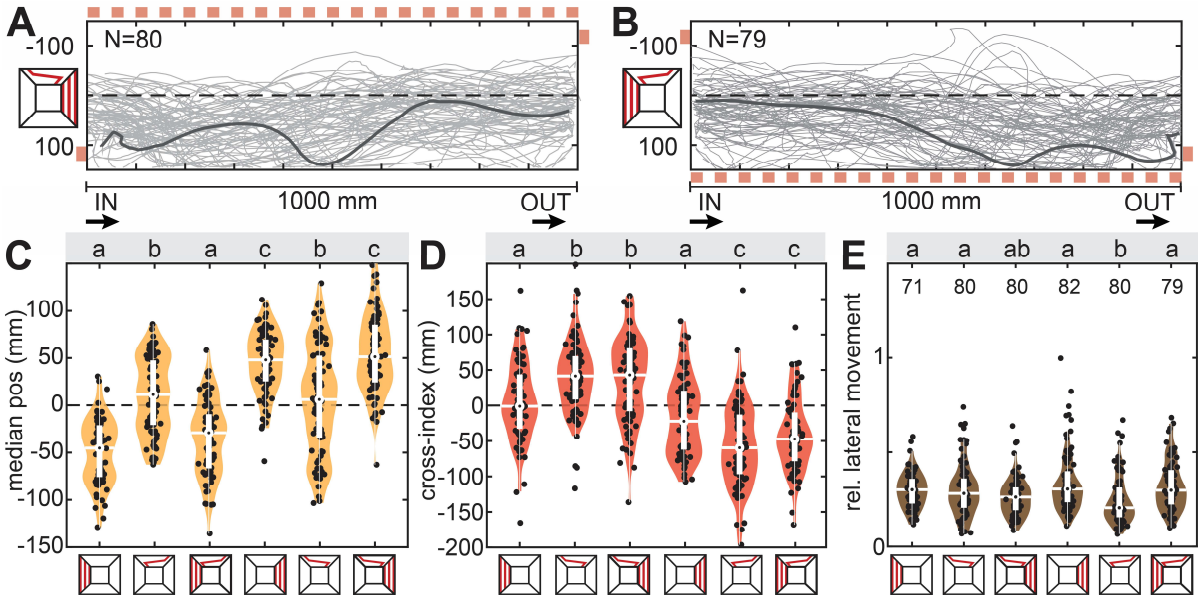

Fig. 3 **Cue conflict: lateral optic flow and dorsal directional cues.**
A, B Flight tracks of hawkmoths presented with a lateral grating inducing translational optic flow, and a dorsal line which switched sides from the first to the last third of the tunnel (from the camera's perspective below the tunnel). N represents the number of flights. The dark grey line highlights a single representative flight track. **C-E** Median position, cross-index and proportion of lateral movement with either grating patterns, the dorsal line stimulus, or a combination of both. Black letters in **C-E** show statistically significant differences in group medians (confidence level: 5%). The white boxplots depict the median and 25% to 75% range, the whiskers represent the data exceeding the box by more than 1.5 interquartile ranges and the violin plots indicate the distribution of the individual data points shown in black.

Cue conflict: lateral optic flow and dorsal directional cues

To test whether and how optic-flow-based avoidance and dorsal direction-following combine to guide the flight position of hawkmoths, we generated a direct conflict by combining a dorsal directional and lateral optic flow cue, which both induce hawkmoths to fly to the same side of

the tunnel (Fig. 3B). For the optic flow cue, we presented vertical red stripes on one tunnel side, which the animals increased their distance to, when presented on their own (Fig. 3D). The dorsal directional cue was a red stripe, which switched tunnel sides towards the optic flow cue in the travel direction of the animals. On its own, this cue induced a cross-over in median tunnel position (Fig. 3E). The lateral grating presented a much higher amplitude of translational optic flow, as well as a higher magnitude of contrast averaged along the length of the tunnel (Fig. 5A,B). When both cues were presented to in combination, we observed mixed responses: the hawkmoths kept their distance to the optic-flow tunnel side with the same magnitude as before (Fig. 3D). Simultaneously, in the now more limited lateral space of half the tunnel width, they performed the switching behaviour, resulting in as high a cross-index as with only the dorsal directional cue alone (Fig. 3E). This is remarkable, because it shows the animals were not simply following the red stripe, as they were not flying under it after the switch to the other tunnel side occurred, but they followed the directional information of this stimulus. Thus, hawkmoths performed both optic-flow-based distance regulation and dorsal directional manoeuvres at the same time, suggesting that these two control systems act in parallel, with similar weights on the final response. Moreover, these weights did not reflect the magnitude of translational optic flow or contrast edges generated by the two types of cues.

To test whether the parallel action of the optic-flow and dorsal directional control systems generalized across tasks and visual stimulation types, we tested hawkmoths with a variant of the optic-flow based lateral distance regulation, and a different contrast pattern: we used a centring task, as frequently used in other species [33-35], by presenting black-and-white checkerboard patterns on both lateral tunnel walls. These were combined with the same dorsal red stripe that changed its lateral position between the first and last third of the tunnel (Fig. S2A). The checkerboard pattern on its own induced a centring response (Fig. S2C), and straight flights with a very low cross-index (Fig. S2D). The dorsal direction-switching red stripe presented on its own resulted in a significantly wider positional distribution across the tunnel width (Fig. S2C), as well as a high cross-index (Fig. S2D). Presenting both cues combined resulted in a response combination of both optic flow and directional control: the animals centred as strongly as in the optic-flow-only condition (Fig. S2C), and their cross-index was similar in direction to the dorsal-directional-only condition (Fig. S2D). The mixed response also manifested in flight speed, which was significantly lower for dorsal-directional-only cues then optic-flow-only cues, and had an intermediate value for the mixed conditions (Fig. S2E).

Thus, hawkmoths performed optic-flow based flight control, including lateral distance regulation and speed control in parallel with dorsal directional manoeuvres across different visual stimuli.

Cue conflict: lateral versus dorsal avoidance

In the previous set of conflict tests, both lateral optic-flow-based distance regulation and dorsal directional responses could be enacted with the same strength as when presented individually. We next tested how the animals responded when dorsal and lateral responses were conflicted, so that it was not possible to enact both to their original magnitude simultaneously. To test this, we set the lateral distancing and dorsal avoidance responses in conflict, by presenting a grating of vertical red stripes on one tunnel wall, which induced the animals to fly on the opposite side of the tunnel (Fig. 4C), coupled with a grating of the same type on one half of the tunnel's ceiling. On its own, the animals avoided the dorsal tunnel coverage by flying on the un-covered tunnel side (Fig. 4C). When combined, we observed a clear hierarchy in responses: the vast majority of animals flew on the side of the tunnel presenting lateral optic flow, thus avoiding the dorsally covered section (Fig. 4C). Yet, the animals' median position was also significantly different from the dorsal-only condition and shifted closer towards the lateral-only condition (Fig. 4C). Moreover, not a single animal had their median flight position

in the covered tunnel side in the dorsal-only condition, but a subset of animals did in the conflict situation (Fig. 4C). Thus, the animals responded to both cues, though with a higher weight for dorsal avoidance. This weighting of responses did not reflect a higher magnitude of translational optic flow or overall contrast in the dorsal versus the lateral visual field (Fig. 5A,B).

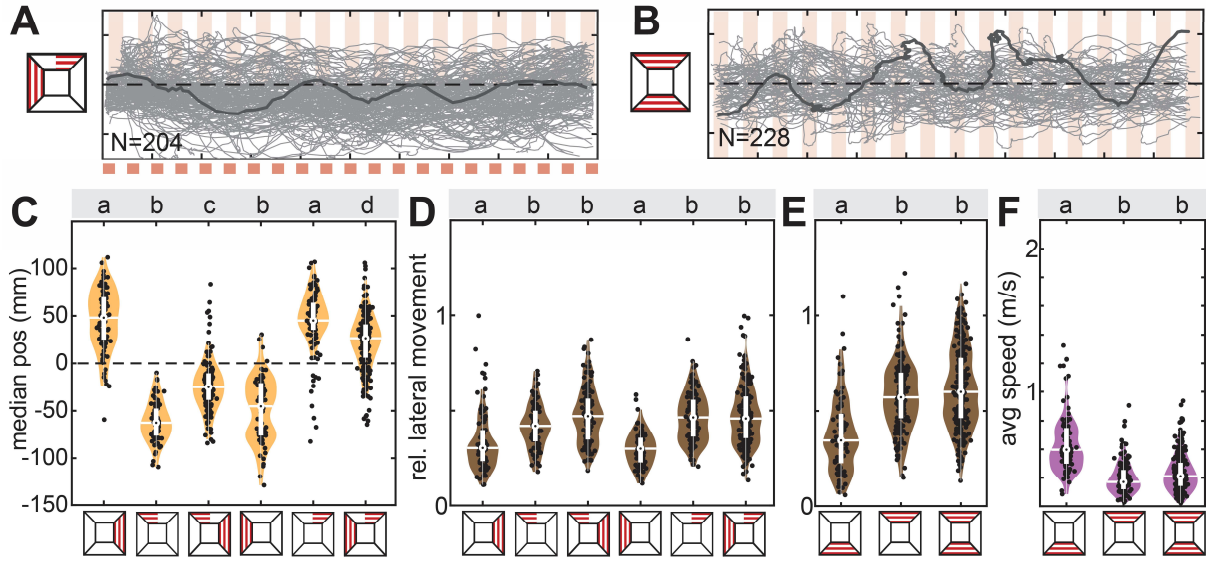

Fig. 4 Cue conflict: lateral versus dorsal avoidance.
Flight tracks of hawkmoths presented with **A** a lateral and a dorsal grating pattern (the latter only spanning one half of the tunnel), and **B** a ventral and dorsal grating pattern, both shown from the camera's perspective below the tunnel. N represents the number of flights. The dark grey line highlights a single representative flight track. **C-F** Median position, proportion of lateral movement and flight speed with either pattern in isolation and in combination. Black letters in **C-E** show statistically significant differences in group medians (confidence level: 5%). The white boxplots depict the median and 25% to 75% range, the whiskers represent the data exceeding the box by more than 1.5 interquartile ranges. The violin plots indicate the distribution of the individual data shown in black.

Noticeably, in these conflict experiments, the lateral movement of the animals (Fig. 4D), and their flight speed (Fig. S3B) was significantly different from the lateral optic flow only condition, but not from the dorsal only condition. High lateral movement and very low speed were highly indicative of the dorsal directional responses and suggest that even in the presence of lateral optic flow in the conflict situation, which supports straight, moderately fast flight, the animals were strongly guided by dorsal cues. Since we previously found that the animals' flight straightness and speed was guided stronger by ventral than lateral optic flow cues [11], we simultaneously presented dorsal and ventral gratings, to test whether dorsal cues would also take over flight guidance in combination with ventral cues. The lateral movement (Fig. 4E) and flight speed (Fig. 4E) in the conflict situation were significantly different from the ventral-only condition, but not significantly different from the dorsal-only one. This demonstrates that in the presence of dorsal contrast cues, the optic-flow based control on flight straightness and speed was taken over by dorsal directional guidance, suggesting the latter has a much greater weight in the control hierarchy. This was observed despite the fact that the ventral gratings generated about 50% stronger translational optic flow than dorsal ones, and a comparable magnitude of contrast cues (Fig. 5B,C). Yet, when analysing the relative flight height, we found that the hawkmoths kept a similar distance to ventral patterns than with ventral cues only, and a significantly higher flight position than with dorsal only cues (Fig. S3C), suggesting that similar to lateral optic flow cues, the perpendicular distance regulation to ventral optic flow cues remained intact when dorsal cues were presented simultaneously.

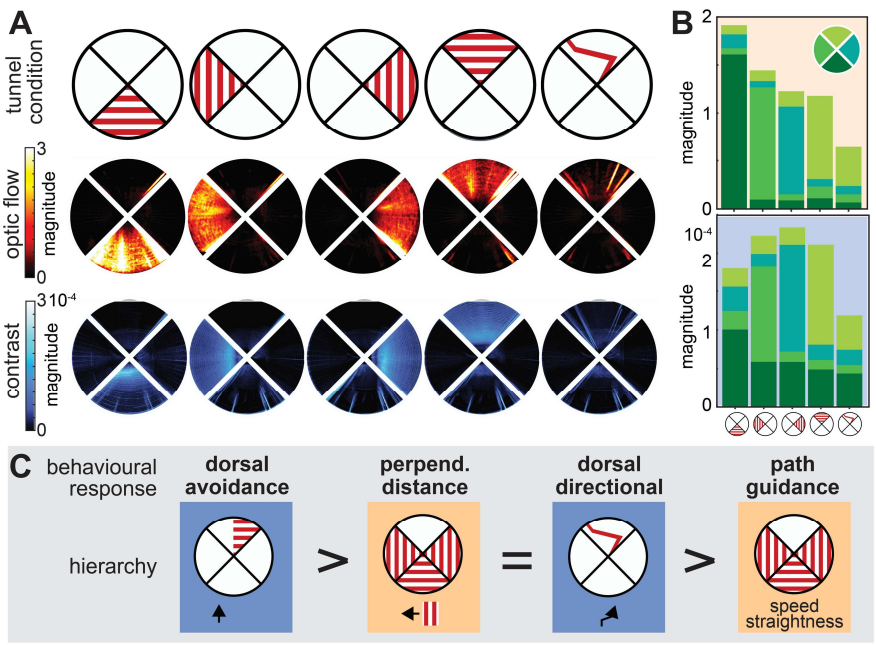

Fig. 5 **Magnitude of translational optic flow and contrast edges in the flight tunnel**. **A** Heatmaps of the magnitude of translational optic flow (middle row) and contrast edges (bottom row) in the different tunnel conditions (top row) used in conflict experiments. **B** Stacked bars present the average magnitude of translational optic flow (top panel) and contrast edges (bottom panel) in each of the four quadrants (ventral, left, right and dorsal) in the five tunnel conditions depicted in **A**. **C** The hierarchy of dorsal directional responses and translational optic flow-based control in the ventrolateral visual field resulting from the conflict experiments.

Discussion

In this study, we characterised the dorsal directional flight response of hummingbird hawkmoths and revealed that it is fundamentally different from the “canonical” optic-flow-based flight control [35]. Using conflict experiments, we demonstrated that optic-flow-based and dorsal directional flight responses act in parallel, though with different relative weights.

The nature of the dorsal response.

Our results demonstrate that the flight responses of hawkmoths to dorsal stimuli did not bear the typical hallmarks of translational optic flow-based flight control, as it is known from bees [15, 16, 21, 24], flies [17-19, 35], or moths [2, 20, 22, 25, 39] to ventrolateral stimuli, and for honeybees to dorsal ones as well [19]. In this paradigm, the magnitude of translational optic flow is thought to be kept constant by a reduction of speed and an increase in perpendicular distance to cues generating optic flow [19, 29]. While the hawkmoths in our experiments slowed down upon perceiving translational optic flow dorsally, they did so much more than for the same stimuli ventrolaterally. Moreover, they aligned with the dominant contrast axis of the stimuli and thus generated a much higher proportion of lateral movement for gratings perpendicular to the tunnel axis. As previously shown in these hawkmoths, high degrees of lateral movement correlate with low flight speed [39], so that the low speed was likely a side effect of the lateral flight, not a response to the optic flow. This also fits the observation that the hawkmoths flew distinctly faster with longitudinal dorsal stripes (Fig. S3C).

Given the hawkmoths’ flight responses, one might hypothesize that contrast in the dorsal visual field induced a behavior aimed at minimizing optic flow, rather than keeping it constant, as they do ventrolaterally. What fits hypothesis is that animals avoided flying under any visual contrast when possible. If this was not possible, they flew under the less-optic flow inducing portions of the tunnel (Fig. 1H). Aligning with the dominant contrast axis could be a strategy to minimize the perceived translational optic flow. However, hawkmoths did not show a perpendicular distance regulation in response to dorsal optic flow cues, as they did for ventrolateral ones. If anything, they flew closer to dorsal stimuli than in a tunnel without patterns (Fig. S2D). This suggests that the dorsal response is not (only) an optic-flow reduction response.

We therefore hypothesise that the dorsal response might be an adaptation to avoid flying under canopies: both the strong avoidance of any dorsal coverage, whether inducing translational optic flow or not, and the alignment with dominant contrast edges, which could be canopy borders, could help to remain flying in the open. The lack of a distance regulation to dorsal optic flow cues might also be explained by a canopy avoidance strategy: if hawkmoths avoided flying under canopies, they would rarely encounter any dorsal optic flow. All the more so, since the natural habitat of these hawkmoths is described as mostly open and semi-open [40]. Moreover, even if a hawkmoth was trapped under dorsal coverage, their most common escape strategy is flying upwards towards a bright spot of sky, which would be impaired if the moths had a regulatory mechanism like for ventrolateral optic flow, which kept them at a safe distance from optic-flow inducing structures.

Integration of the dorsal system with optic flow-based flight control.

For ventrolateral flight responses of hummingbird hawkmoths, we confirmed previous studies, which show typical translational optic-flow-based flight regulation [11, 27, 28]. Our vertical distance measure added a final puzzle piece to this and confirmed that as for lateral cues, hummingbird hawkmoths also increased their perpendicular distance to ventral translational optic flow (Fig. S1).

Our results suggest that this optic-flow-based flight control system acts in parallel to the dorsal canopy avoidance system, because stimuli in both the dorsal and ventral visual field created mixed responses, which are only possible if both systems were active at the same time. Our series of conflict experiments revealed the following hierarchy between the two systems: the highest weight was given to the avoidance of dorsal coverage. This behaviour occurred simultaneously with the optic-flow based distance regulation, but reduced the latter's impact when set in direct conflict. Ventrolateral distance regulation to optic flow operated at a similar weight to the body alignment with dorsal contrast edges, and produced mixed results of similar magnitudes as the behaviours on their own, even when the presented contrast edges had a lower stimulus magnitude.

Optic-flow based speed regulation had the lowest weights in this hierarchy. Our results also question whether hawkmoths indeed use a combination of flight speed and distance regulation to retain a constant optic flow percept, as has been suggested in other insects [19, 29, 41]. Indeed, the hawkmoths in our experiments kept very similar distances to ventral and lateral optic flow, despite drastically different flight speeds (which were induced by the presence or absence of dorsal cues, Fig. 3C, 4F, S3C). Instead, these results suggest that the animals can measure the distance to optic-flow-generating textures in their ventrolateral visual field, and subsequently adjust their distance, independently of speed. This could be possible using optic flow divergence, the perceived expansion and contraction caused by flight movements towards and away from a texture [42, 43]. If hawkmoths measured the distance to objects in their ventrolateral visual field using expansion cues, and separately attempted to retain the perceived optic flow constant via adjustments of flight speed, this would explain the two modules having different weights in the control hierarchy and operating separately from each other in the behavioural experiments.

The ecological relevance of the dorsal and ventrolateral flight control systems.

If one interprets the observed flight control hierarchy in terms of ecological function, the highest priority for hummingbird hawkmoths would is not to fly into foliage. To this aim, they avoid any dorsal coverage. This aim operates in parallel with keeping a distance to ventrolateral texture, to remain at a safe distance from potential obstacles. Interestingly, the tolerated distance to ventrolateral texture was reduced at the benefit of avoiding dorsal coverage. It remains to be tested if there is a minimum tolerated distance that the animals consider to be safe.

The dorsal contrast avoidance behaviour has not yet been observed in other insects. It is possible that the lifestyle of the insects tested previously is more tolerant of surrounding foliage than that of hawkmoths: honeybees naturally build their nests in trees, while bumblebee nests in the ground might be surrounded by trees or shrubs. The animals thus encounter, and might also use, surrounding foliage, including dorsal coverage, during their daily navigation to and from the nest [44, 45]. They might therefore be tolerant of dorsal contrast cues, and because they encounter them frequently, use their translational optic flow component to guide flight in the same way across the entire visual field. To understand whether using or avoiding dorsal optic flow is indeed coupled with insect habitat and lifestyle, comparative studies are required, particularly of hawkmoth species that live in forest versus open environments [40], and of other insects that live in similar open habitats to hummingbird hawkmoths.

One other explanation for the observation that honeybees keep the perceived translational optic flow constant in either part of their visual field by adjusting distance and speed [19] is odometry. Honeybees have been shown to measure the distance of their path to food sources using the translational optic flow integrated during their flight, and communicate this information to nestmates to guide them to the same food source [46, 47]. In order for this strategy to work, reproducible optic flow on consecutive flights is required – which is not

straightforward, since different landscape structures, and flight at different speeds and distances from the surrounding structure, generate different perceives magnitudes of translational optic flow [48] (Fig. 1B), resulting in different perceived lengths of path travelled. One way to generate reliable distance measures is to keep perceived translational optic flow constant – which might be a key function for the optic flow regulator observed in bees. This hypothesis fits well with the observation that honeybees, when trained to fly close to the floor or ceiling of a tunnel on the way to a food source, or one of its walls [49], will repeat this strategy when their entrance into the tunnel, or the tunnel shape changes [50], thus preserving the rate of optic flow they perceived when learning their way to the food source. Thus, in honeybees, keeping the perceived translational optic flow constant across the entire visual field might have less to do with flight guidance or safety, and more with keeping a reliable translational optic flow percept for odometry. This would also explain the differences to hawkmoths, which are not known to path integrate, and demonstrate that retaining safe flight is possible without a constant optic flow strategy. Comparing path integrating and non-path integrating insects would reveal whether the optic flow regulator strategy involving speed and distance regulation serves path integration rather than flight control.

General takeaways for parallel control in sensory systems.

Beyond the mechanisms of flight control in insects, this study also provides fundamental insights into strategies of partitioning the visual field, and how parallel pathways are integrated for a robust behavioural response. The benefit of our study system is that the same cues activate different control pathways in different regions of the visual field, so that the weights of the integration hierarchy can directly be compared (unlike for different qualitative types of visual cues, or different sensory modalities, where comparing the perceived magnitude of the different cues is not straightforward). What these experiments show is that the partitioning of the visual field follows the probability with which these cues occur in the animals' habitat: translational optic flow occurs more frequently and with a higher magnitude in the ventrolateral visual field than in the dorsal one (Fig. 1B). This is mirrored in the receptive areas of the optic-flow-based flight guidance, while canopy avoidance responses occur exclusively to cues in the dorsal visual field – where contrast cues are the strongest, due to the backlighting of the sky (Fig. 1B). It remains to be tested at what elevation the visual field partitions, and whether there is an area of overlap, in which either behaviour could be elicited, as is the case for landing and predator avoidance towards looming stimuli in fruit flies [36].

Contrary to the visual field partitioning by the stimulus statistics in natural habitats [7-9], the integration hierarchy does not follow this strategy. In the natural habitats of hawkmoths, dorsal coverage is much less frequent that ventrolateral structures generating translational optic flow, yet the hawkmoths responded with a much higher weight to the former. Moreover, in our flight tunnel experiments, the animals responded with the same or higher weights to dorsal cues, which had a lower magnitude of translational optic flow and contrast than the same cues in the ventrolateral visual field. This differs from other sensory integration strategies, which are generally thought to weigh the modality highest which carries the highest reliability or the most information [37, 38]. The strategy emerging for flight control in the hummingbird hawkmoth is one of reacting to the most immediate "danger" to the animal: the stimuli that carry the biggest potential threat for the animals' (flight) safety are weighed highest, while in the event of these stimuli, the tolerance for other risks (such as flying closely to lateral structures) is increased. Thus, dorsal contrast cues might not constitute the most frequent or reliable input, but the one with the highest priority in terms of the animals' safety, and therefore are assigned the highest weights in the control hierarchy.

Thus, to understanding parallel processing strategies, and the integration of parallel information for behavioural guidance, both the prevalence, magnitude, and reliability of the input statistics are important, as well as the relevance of these stimuli to the particular behaviour of the animals. In the case of flight control in the hummingbird hawkmoth, prevalence shapes the partitioning of the visual field, while relevance determines the integration hierarchy of the parallel pathways.

Material and Methods

Optic flow imaging

Imaging of natural scenes

To film a 180° frontal visual field panorama, we used the imaging setup designed and described in detail in [11]. In short, we captured translational optical flow in videos using a full-HD digital camera (USBFHD01M, ELP), equipped with a 185° fisheye lens (1.08 mm focal length, BL-5MP010820MP13IR, Vision Dimension). The camera was attached to the front of a 19 V-powered linear actuator with 70 cm extension (Bewinner) and a movement speed of 12 mm/s. This system was mounted onto a tripod ca. 1 m above ground and captured the visual scenery during 70 cm of horizontal forward movement at a constant distance to the ground. Videos were captured with the open-source software ContaCam 7.9.0 software (Contaware) at a rate of 30 frames per second. To correct undesired rotation in the videos, generated by the linear acturator's movement, we tracked three horizontally aligned landmarks in outdoor recordings, which were attached to a second tripod and positioned 3 m in front of the camera, to take up only a small portion of the visual field. The landmark positions were used to correct image rotations in Matlab 2020a (The Mathworks). Any remaining instability in video position was removed with the video stabilization filter Deshaker 3.1 (Gunnar Thalin; guthspot.org) in VirtualDub v1.10.4 (virtualdub.org).

Videos were collected on sunny days (individual clouds were tolerated) in three different types of natural habitats: open, semi-open, closed. Open habitats had no bushes or trees within 20 m of the camera position; semi-open environments had different combinations of shrubs and trees but no complete cover overhead, and the closed habitats were filmed under closed tree canopies (Fig. 1C). We collected videos in three different locations of each habitat type, and within each of the location we filmed at three different perspectives to not bias the analysis with a specific view (with exception of one location in the open habitat type, where only two perspectives were filmed, resulting in N=8 for open habitats, and N=9 for semi-open and closed ones).

In the flight tunnel setup, the camera was positioned centrally with equal distance to all walls and extended from one tunnel entrance 70 cm into the flight tunnel.

Analysis of optic-flow fields and contrast features

The dense optical flow in the videos was estimated by the Gunnar Farnebäck method [51], using Open CV with Python 3.7.6, which computed an optic-flow vector (angle and magnitude) for every pixel in each frame. In Matlab 2022a, we then used a filter to pass only the optic flow vectors that corresponded to translational optic flow along the camera's trajectory. In our setup, the viewing axis and the direction of camera travel were the same, thus translational optic flow was represented in vectors with angles radially oriented around the image centre. The mean magnitude of these vectors was then calculated for each pixel of the video. All pixel magnitudes of each video of a scene were averaged and extracted in one of four quadrants (dorsal, ventral, left lateral, right lateral) for subsequent analysis.

We extracted contrast edges using the Matlab 2022a inbuilt function "edge", using a Prewitt filter, and variable contrast threshold (0.01, 0.025, 0.05, 0.1 and 0.5). Each extracted edge in each frame of each video was scaled by the highest threshold required to detect it. All contrast edges of each video of a scene were averaged and extracted in one of four quadrants (dorsal,

ventral, left lateral, right lateral) for subsequent analysis. For natural visual scenes, the lateral quadrants were averaged and combined, while they were left separate for the analysis of optic flow and contrast in the tunnels, to allow for a detailed assessment of the employed tunnel conditions.

Statistical analysis of the magnitude of optic flow and contrast edges across habitat types (*open*, *semi*, *closed*) and quadrants of the visual field (*ventral*, *lateral*, *dorsal*) was performed in R 4.3.1, using a linear mixed-effects model (*lm4* package) with scenes within conditions as random effects, using the formula

$$\text{magnitude} \sim \text{habitat} \times \text{quadrant} + (1 \mid \text{scene})$$

We confirmed that the full model had a lower AIC and deviance than the null model with only random effects, as well as models with either factor only and random effects, before continuing pairwise posthoc tests (*emmeans* package, default correction: Tukey).

Behavioural experiments

Animals

Adult male and female *Macroglossum stellatarum* (Linnaeus 1758) were raised on their native host plant *Gallium* sp. The eclosed adults (both male and female) were allowed to fly and feed from artificial feeders in flight cages (60×60×60 cm, length×width×height) on a 14 h:10 h light:dark cycle for at least one day before experiments began.

Flight tunnel setup

Details of the experimental setup and data analysis have been described previously [11, 39] and will be briefly summarised. Two flight cages (60×60×60 cm, length×width×height) were connected by a Perspex flight tunnel (100×30×30 cm, length×width×height, Fig. 2A,B). The tunnel and cages were illuminated by fluorescent tubes with a daylight-like spectrum (Osram L 18W/965 Biolux Tageslicht G13). A white screen in the middle of the left flight cage (60 cm high, 45 cm wide) obstructed the view into the cage when animals were flying in the tunnel. The feeders were hidden behind this screen. A camera (Playstation Eye, PS3, Sony) was positioned 1.5 m below the tunnel to film its entire length. It was controlled by ContaCam 7.9.0 beta7 software (Contaware) in motion detection mode at a rate of 50 frames per second and an aspect ratio of 640×480 pixels.

Visual stimulation

To disguise the visual panorama above the tunnel, white felt was placed on top of the tunnel ceiling as a diffuser. Gauze (Gazin Verbandmull 8-fach, Lohmann & Rauscher) was placed on the tunnel floor to avoid light reflections and access to the visual panorama below the tunnel (Fig. 2A). It allowed the camera mounted below the tunnel to film through it. The tunnel side walls were lined with 5% nominal contrast checkerboard patterns (13.9 mm side length, equivalent to a viewing angle of 5.3° from the centre of the tunnel) for all experimental conditions. This provided sufficient visual feedback to reduce collisions of the animals with the walls, while at the same time minimising the classical hallmarks of translational optic flow flight responses [11]. For stimulation, we used transparent red plastic sheets (Neewer, #10088988), through which the animals could be filmed and tracked using the red channel of the RGB videos. All patterns were mounted so that they were presented on top of the gauze, diffuser and 5% checkerboard patterns. We constructed grating patterns out of 3 cm wide stripes of

the red sheet, alternating with no stripes. These either spanned the entire 30 cm of one tunnel side, or only 15 cm of the ceiling or floor. Additionally, we also constructed 6 cm and 1.5 cm wide striped gratings, to test the reliance of the dorsal and ventral responses on the stripe frequency. In addition to the grating stimuli, we constructed a directional stimulus out of the red sheets, which was 3 cm wide, and consisted of a 33 cm straight section on either tunnel side mounted 5 cm from the edge of the tunnel at opposite sides, and a connecting diagonal in the central 33 cm of the tunnel, as well as a version of this stimulus with repetitions of the stripe every 3 cm (Fig. 2G). We anticipate the red stimuli to only weakly activate the green photoreceptors of *M. stellatarum*, and thus appear as a dark feature on top of a brighter background.

Experimental procedure

Prior to experiments, thirty to forty hummingbird hawkmoth individuals were accustomed to the setup for two days as described in [11]. Briefly, during training, the tunnel side walls were lined with a black and white chequerboard pattern for optimal visual feedback. On the first day, feeders were presented freely visible in the left flight cage, and the animals were moved between the left and right flight cage repeatedly. The following day, the feeders were hidden behind a white screen, and the animals were regularly moved back to the right cage which had no feeders, to encourage the use of the tunnel.

After familiarisation with the setup, experiments started with feeders in the left flight cage, which were obstructed from view. Animals that were resting in the left cage were moved back to the right cage (without feeders) every two hours between 9.00 and 17.00. The visual stimuli were changed daily or, if too few flights were recorded in that period, every two days. Flights through the tunnel were filmed continuously, although the first hour after pattern changes was not analysed to allow hawkmoths to adjust to the new visual scenario. To exclude side biases, we performed all directional experiments with patterns on either side of the tunnel.

Video analysis

As detailed previously [39], not all individuals of *M. stellatarum* traverse the tunnel in a directed fashion. Therefore, we only analysed complete flight tracks from the right to the left flight cage that did not contain landing attempts. Moreover, the tunnel had to be free of other hawkmoths. The flight tracks were then digitised using custom-written software in Matlab R2022a, which detected the animals based on frame-to-frame image differences. The resulting image differences contained the silhouette of the hawkmoths, which was used to extract the area covered by each moth in each frame, using the Matlab inbuilt function *regionprops*. The animals' current position was extracted as the centroid of each detected area. The size of the area was used as a proxy for the animals' height in the tunnel: the larger the area, the closer the animals flew to the camera, which was positioned under the tunnel; thus, the closer they flew towards the bottom of the tunnel. While this measure did not provide exact flight height in the tunnel, it could be used to analyse trends in the average height the moths' traversed the tunnel at (Fig. S1D,G,H and S3C). The digitised tracks were analysed in the central 80 cm of the tunnel, to exclude the portions of flight where cues from the flight cages could have been visible. We quantified the median of the lateral positions (along the width of the tunnel) of each flight track, the median of the frame-to-frame speed of each flight track, the proportion of lateral movement (as the median of the ratio of movement along the lateral to the longitudinal axis of the tunnel) and a cross-index (by subtracting the lateral position of the animal before exiting – 600 to 800 mm - from the one after entering the tunnel – 200 to 400 mm, see also Fig. 2C).

Statistical analysis and presentation

The median lateral position in the tunnel, lateral movement, cross-position index and tracking area of individual flights were compared across conditions, using ANOVA with Tukey-Kramer-corrected post-hoc comparisons, if the normality of all residuals was confirmed. If not, a Kruskal–Wallis test with Tukey-Kramer-corrected post-hoc comparisons was performed. The nature of the test is indicated in the statistical results files in the data repository. If not indicated otherwise, statistical results are shown with a significance level of 5%. The variance in the median lateral position (in other words, the spread of the median flight position) was statistically compared between the groups using the pairwise Brown–Forsythe test), as a measure for the strength of centring in the tunnel.

For the graphical data summary, the individual data points were spread around the x-axis position of the group by drawing from a Gaussian distribution, which was scaled to 0.05 x-axis units. The whiskers of the boxplots represent the data range extending more than 1.5 interquartile ranges from the box limits. The violin plots indicate the distribution of the individual data points; their smoothing kernel was set to 0.04 times the range of each group of data.

Author Contributions Conceptualization: A.S.; Methodology: A.S., R.B.; Validation: A.S., R.B.; Formal analysis: A.S., R.B., R.G.; Investigation: R.B., R.G.; Resources: A.S.; Data curation: A.S., R.B.; Writing - original draft: A.S., R.B.; Writing - review & editing: A.S., R.B., R.G.; Visualization: A.S., R.B.; Supervision: A.S.; Funding acquisition: A.S.

Acknowledgements We acknowledge funding to A.S. by the German Research Council (STO 1255 2-1), and to A.S. and R.B. by the Young Scholar Fund of the University of Konstanz. We thank James Foster for suggestions on the statistical analysis.

Data Availability

Source data for the behavioural experiments, as well as natural scenes and tunnel pattern imaging, and all statistical results files, are available from https://figshare.com/s/e680da3be83fe172a5e4

Custom-written analysis code is available from https://github.com/stoeckllab/Bigge_et_al_2024

References

[1] Duistermars, B.J. and Frye, M.A. (2008). Crossmodal Visual Input for Odor Tracking during Fly Flight. Current Biology *18*, 270–275.

[2] Vickers, N.J. and Baker, T.C. (1994). Visual feedback in the control of pheromone-mediated flight of *Heliothis virescens* males (Lepidoptera: Noctuidae). J. Insect. Behav. *7*, 605–632. https://doi.org/10.1007/BF01997435.

[3] Fox, J.L. and Frye, M.A. (2014). Figure-ground discrimination behavior in *Drosophila*. II. Visual influences on head movement behavior. J. Exp. Biol. *217*, 570–579. http://-dx.doi.org/10.1242/jeb.080192.

[4] Frighetto, G. and Frye, M.A. (2023). Columnar neurons support saccadic bar tracking in *Drosophila*. eLife *12*.

[5] Nassi, J.J. and Callaway, E.M. (2009). Parallel processing strategies of the primate visual system. Nat. Rev. Neurosci. *10*, 360–372.

[6] Doudlah, R., Chang, T.Y., Thompson, L.W., Kim, B., Sunkara, A., and Rosenberg, A. (2022). Parallel processing, hierarchical transformations, and sensorimotor associations along the 'where' pathway. eLife *11*.

[7] Baden, T., Schubert, T., Chang, L., Wei, T., Zaichuk, M., Wissinger, B., and Euler, T. (2013). A tale of two retinal domains: near-optimal sampling of achromatic contrasts in natural scenes through asymmetric photoreceptor distribution. Neuron *80*, 1206–1217.

[8] Hornstein, E.P., O'Carroll, D.C., Anderson, J.C., and Laughlin, S.B. (2000). Sexual dimorphism matches photoreceptor performance to behavioural requirements. Proc. R. Soc. B. *267*, 2111–2117. http://dx.doi.org/10.1098/rspb.2000.1257.

[9] Turner, M.H., Giraldo, L.G.S., Schwartz, O., and Rieke, F. (2019). Stimulus- and goal-oriented frameworks for understanding natural vision. Nat. Neurosci. *22*, 15–24.

[10] Koenderink, J.J. (1986). Optic flow. Vision Res. *26*, 161–179.

[11] Bigge, R., Pfefferle, M., Pfeiffer, K., and Stöckl, A. (2021). Natural image statistics in the dorsal and ventral visual field match a switch in flight behaviour in hawkmoths. Curr. Biol. *31*, R280 – R281.

[12] Hölldobler, B. (1980). Canopy orientation: a new kind of orientation in ants. Science *210*, 86–88.

[13] Calow, D. and Lappe, M. (2007). Local statistics of retinal optic flow for self-motion through natural sceneries. Network: Computation in Neural Systems *18*, 343–374.

[14] Zanker, J.M. and Zeil, J. (2005). Movement-induced motion signal distributions in outdoor scenes. Network: Computation in Neural Systems *16*, 357–376.

[15] Baird, E., Srinivasan, M.V., Zhang, S., and Cowling, A. (2005). Visual control of flight speed in honeybees. J. Exp. Biol. *208*, 3895–3905.

[16] Baird, E., Kornfeldt, T., and Dacke, M. (2010). Minimum viewing angle for visually guided ground speed control in bumblebees. J Exp Biol *213*, 1625–1632.

[17] David, C.T. (1982). Compensation for height in the control of groundspeed by *Drosophila* in a new, 'barber's pole' wind tunnel. J. Comp. Physiol. A. *147*, 485–493. https://-doi.org/10.1007/BF00612014.

[18] Fry, S.N., Rohrseitz, N., Straw, A.D., and Dickinson, M.H. (2009). Visual control of flight speed in *Drosophila melanogaster*. J. Exp. Biol. *212*, 1120–1130.

[19] Portelli, G., Ruffier, F., Roubieu, F.L., and Franceschini, N. (2011). Honeybees' speed depends on dorsal as well as lateral, ventral and frontal optic flows. PLoS One *6*, e19486.

[20] Willis, M.A. and Carde, R.T. (1990). Pheromone-modulated optomotor response in male gypsy moths, *Lymantria dispar* L.: Upwind flight in a pheromone plume in different wind velocities. J. Comp. Physiol. A. *167*, 699. http://dx.doi.org/10.1007/BF00192664.

[21] Dyhr, J.P. and Higgins, C.M. (2010). The spatial frequency tuning of optic-flow-dependent behaviors in the bumblebee *Bombus impatiens*. J. Exp. Biol. *213*, 1643–1650.

[22] Kennedy, J.S. and Marsh, D. (1974). Pheromone-Regulated Anemotaxis in Flying Moths. Science *184*, 999–1001.

[23] Kern, R., Boeddeker, N., Dittmar, L., and Egelhaaf, M. (2012). Blowfly flight characteristics are shaped by environmental features and controlled by optic flow information. J. Exp. Biol. *215*, 2501–2514.

[24] Kirchner, W.H. and Srinivasan, M.V. (1989). Freely flying honeybees use image motion to estimate object distance. Naturwissenschaften *76*, 281–282. http://dx.doi.org/-10.1007/BF00368643.

[25] Kuenen, L.P.S. and Baker, T.C. (1982). Optomotor regulation of ground velocity in moths during flight to sex pheromone at different heights. Physiol Entomol *7*, 193–202.

[26] Portelli, G., Ruffier, F., and Franceschini, N. (2010). Honeybees change their height to restore their optic flow. Journal of Comparative Physiology A *196*, 307–313.

[27] Grittner, R., Baird, E., and Stöckl, A. (2021). Spatial tuning of translational optic flow responses in hawkmoths of varying body size. J Comp Physiol A *208*, 279–296.

[28] Stöckl, A.L. and Kelber, A. (2019). Fuelling on the wing: sensory ecology of hawkmoth foraging. J. Comp. Physiol. A Neuroethol. Sens. Neural. Behav. Physiol. *205*, 399–413.

[29] Franceschini, N., Ruffier, F., and Serres, J. (2007). A Bio-Inspired Flying Robot Sheds Light on Insect Piloting Abilities. Current Biology *17*, 329–335.

[30] Linander, N., Baird, E., and Dacke, M. (2017). How bumblebees use lateral and ventral optic flow cues for position control in environments of different proximity. J. Comp. Physiol. A Neuroethol. Sens. Neural. Behav. Physiol. *203*, 343–351.

[31] Linander, N., Dacke, M., and Baird, E. (2015). Bumblebees measure optic flow for position and speed control flexibly within the frontal visual field. J. Exp. Biol. *218*, 1051–1059.

[32] Mazo, C. and Theobald, J.C. (2014). To keep on track during flight, fruitflies discount the skyward view. Biol. Lett. *10*, 20131103.

[33] Collett, T.S. (2002). Insect vision: controlling actions through optic flow. Curr. Biol. *12*, R615–R617.

[34] Egelhaaf, M. (2023). Optic flow based spatial vision in insects. Journal of Comparative Physiology A *209*, 541–561.

[35] Srinivasan, M.V., Poteser, M., and Kral, K. (1999). Motion detection in insect orientation and navigation. Vision Res. *39*, 2749–2766.

[36] Tammero, L.F. and Dickinson, M.H. (2002). Collision-avoidance and landing responses are mediated by separate pathways in the fruit fly, *Drosophila melanogaster*. J. Exp. Biol. *205*, 2785–2798.

[37] Dacke, M., Bell, A.T.A., Foster, J.J., Baird, E.J., Strube-Bloss, M.F., Byrne, M.J., and el Jundi, B. (2019). Multimodal cue integration in the dung beetle compass. Proceedings of the National Academy of Sciences *116*, 14248–14253.

[38] Stöckl, A., Heinze, S., Charalabidis, A., El Jundi, B., Warrant, E., and Kelber, A. (2016). Differential investment in visual and olfactory brain areas reflects behavioural choices in hawk moths. Sci. Rep. *6*, 26041. http://dx.doi.org/10.1038/srep26041.

[39] Stöckl, A., Grittner, R., and Pfeiffer, K. (2019). The role of lateral optic flow cues in hawkmoth flight control. J. Exp. Biol. *222*, jeb199406.

[40] Pittaway, A. (1993). The Hawkmoths of the Western Palearctic (Colchester, UK: Harley Books).

[41] Serres, J.R. and Ruffier, F. (2017). Optic flow-based collision-free strategies: From insects to robots. Arthropod. Struct. Dev. *46*, 703–717.

[42] Bergantin, L., Harbaoui, N., Raharijaona, T., and Ruffier, F. (2021). Oscillations make a self-scaled model for honeybees' visual odometer reliable regardless of flight trajectory. Journal of The Royal Society Interface *18*, 20210567.

[43] Ho, H.W., de Croon, G.C., and Chu, Q. (2017). Distance and velocity estimation using optical flow from a monocular camera. International Journal of Micro Air Vehicles *9*, 198–208.

[44] Collett, T.S. and Baron, J. (1994). Biological compasses and the coordinate frame of landmark memories in honeybees. Nature *368*, 137–140.

[45] de Ibarra, N.H., Philippides, A., Riabinina, O., and Collett, T.S. (2009). Preferred viewing directions of bumblebees (*Bombus terrestris* L.) when learning and approaching their nest site. Journal of Experimental Biology *212*, 3193–3204.

[46] Srinivasan, M.V., Zhang, S.W., and Bidwell, N.J. (1997). Visually Mediated Odometry in Honeybees. Journal of Experimental Biology *200*, 2513–2522.

[47] Srinivasan, M.V., Zhang, S., Altwein, M., and Tautz, J. (2000). Honeybee navigation: nature and calibration of the "odometer". Science *287*, 851–853.

[48] Tautz, J., Zhang, S., Spaethe, J., Brockmann, A., Si, A., and Srinivasan, M. (2004). Honeybee Odometry: Performance in Varying Natural Terrain. PLoS Biology *2*, e211.

[49] Serres, J.R., Masson, G.P., Ruffier, F., and Franceschini, N. (2008). A bee in the corridor: centering and wall-following. Naturwissenschaften *95*, 1181–1187.

[50] Portelli, G., Serres, J.R., and Ruffier, F. (2017). Altitude control in honeybees: joint vision-based learning and guidance. Scientific Reports *7*.

[51] Farnebäck, G. (2003). Two-frame motion estimation based on polynomial expansion. In Scandinavian Conference on Image Analysis (Springer), pp. 363–370.

Supplementary Figures

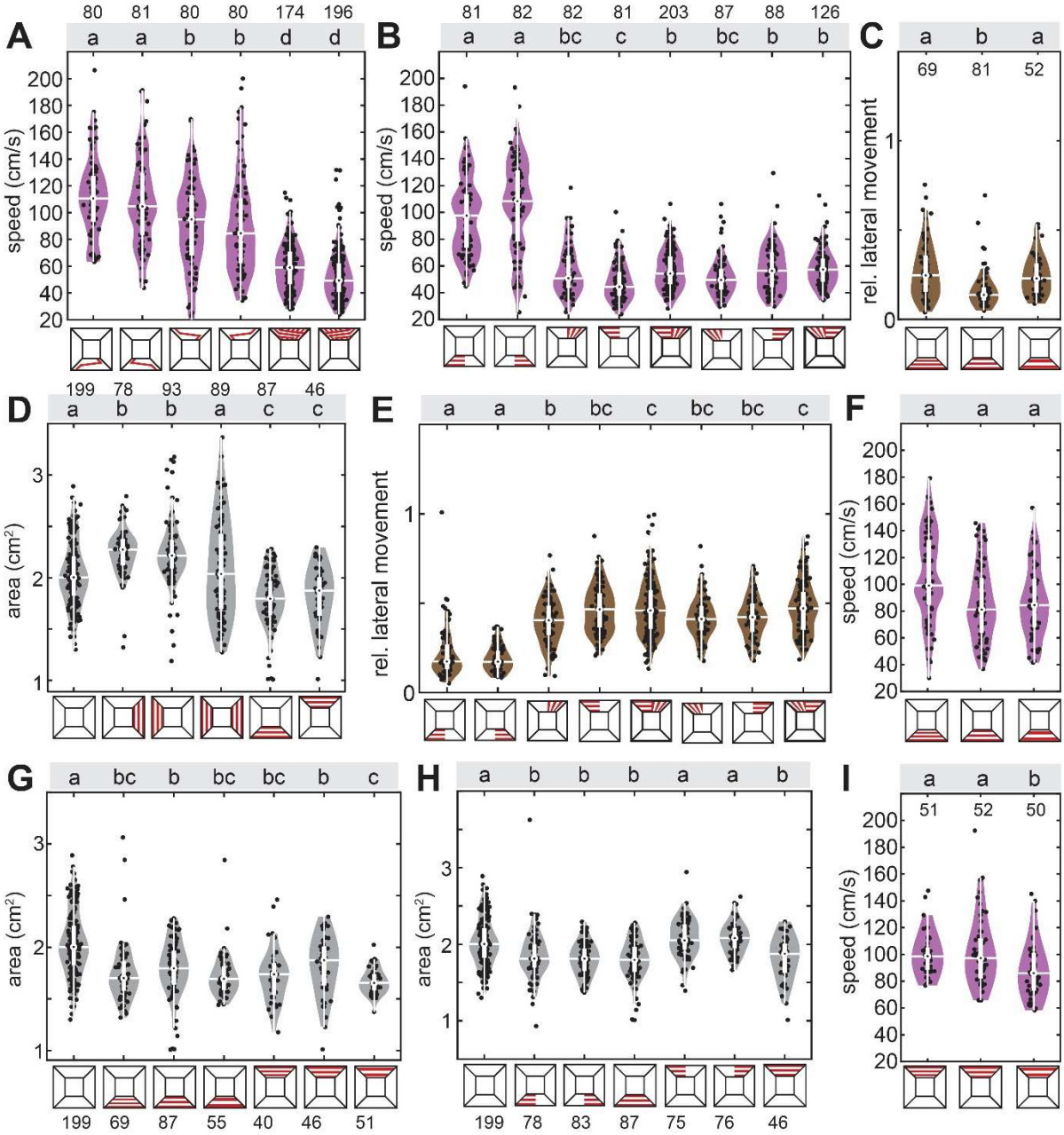

Fig. S1 **Optic flow based flight control and dorsal directional responses.**
A Average speed of flight paths with a red stripe which changed its position in the central third of the tunnel, crossing from one tunnel side to the other. The last two conditions present a version of this stripe, which repeated at the same frequency as the grating patterns. **B,E** Average speed and proportion of lateral movement of flight paths with gratings perpendicular (generating strong translational optic flow) and parallel (weak translational optic flow) to the tunnel's longitudinal axis, covering one side of either the tunnel ceiling or floor. **C, F, I** Proportion of lateral movement and average speed with gratings of different spatial frequencies (repeating every 3 cm, 6 cm and 12 cm), mounted on the tunnel floor or ceiling, respectively. **D, G, H** Area of hawkmoth silhouette in tunnel videos, as a measure of their flight height above the tunnel floor (the smaller the area, the higher the hawkmoths) with grating patterns on either tunnel side (**D**), gratings of various spatial frequencies mounted ventrally and dorsally (**G**) and gratings covering half the tunnel or the full tunnel ventrally and dorsally (**H**). Black letters show statistically significant differences in group medians (confidence level: 5%). The white boxplots depict

the median and 25% to 75% range, the whiskers represent the data exceeding the box by more than 1.5 interquartile ranges and the violin plots indicate the distribution of the individual data points shown in black.

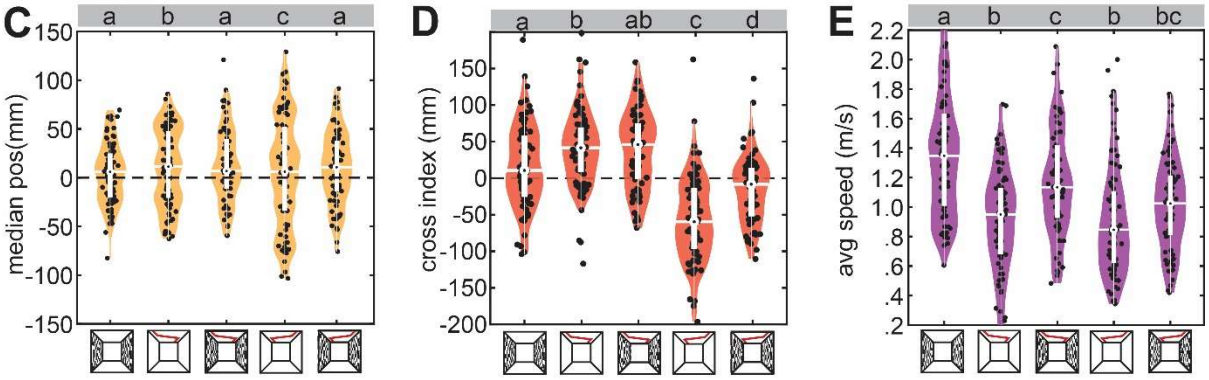

Fig. S2 Cue conflict: lateral optic flow and dorsal directional cues.
A-C Median lateral position, cross-index and average speed of flight paths with a red stripe which changed its position in the central third of the tunnel, crossing from one tunnel side to the other, and a 50% contrast checkerboard pattern on both lateral tunnel sides, presented individually and in combination. Black letters show statistically significant differences in group medians (confidence level: 5%). The white boxplots depict the median and 25% to 75% range, the whiskers represent the data exceeding the box by more than 1.5 interquartile ranges and the violin plots indicate the distribution of the individual data points shown in black.

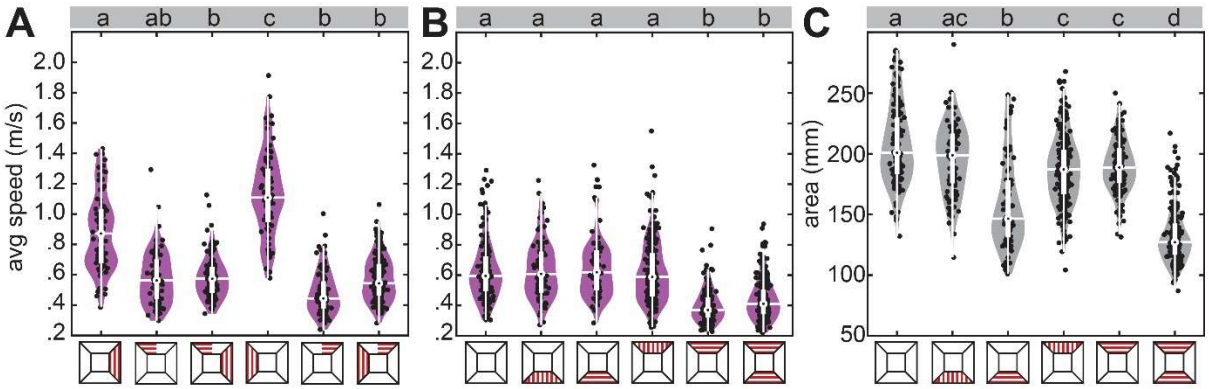

Fig. S3 Cue conflict: lateral distance regulation versus dorsal avoidance. A Average speed of flight paths with lateral gratings and dorsal gratings covering half the tunnel, presented individually and in combination. **B** Average area of hawkmoths as a readout for flight height (the smaller the area, the higher the hawkmoths in the tunnel) in videos with dorsal and ventral longitudinal and perpendicular gratings. Black letters show statistically significant differences in group medians (confidence level: 5%). The white boxplots depict the median and 25% to 75% range, the whiskers represent the data exceeding the box by more than 1.5 interquartile ranges and the violin plots indicate the distribution of the individual data points shown in black.

Supplementary Tables

Table S1 Summary of visual stimulation conditions (labels as used in data repository https://figshare.com/s/e680da3be83fe172a5e4), and number of flight tracks per condition.

	Condition label	**number of flight tracks (N)**
	none	160
	right OF	81
	left OF	79
	lateral OF	80
	ventral OF	81
	dorsal OF	82
	ventral switch lr	80
	ventral switch rl	81
	dorsal switch lr	80
	dorsal switch rl	80
	dorsal switchgrating lr	174
	dorsal switchgrating lr	196
	none2	156
	ventral half OF l	81
	ventral half OF r	82
	dorsal half long l	87
	dorsal half long r	82
	dorsal half OF l	81
	dorsal half OF r	88
	dorsal half OF l long r	203

	dorsal half long l OF r	126
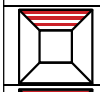	dorsal OF 3cm	51
	dorsal OF 12cm	50
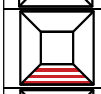	ventral OF 3cm	69
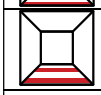	ventral OF 12cm	52
	dorsal switch lr right OF	80
	dorsal switch rl left OF	79
	dorsal half OF l right OF	126
	dorsal half OF r left OF	203
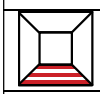	ventralOF2	69
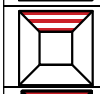	dorsalOF2	157
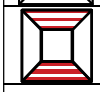	dorsal OF ventral OF	227
	lateral checker	81
	lateral checker switch lr	73
	lateral checker switch rl	67
	ventral long	69
	dorsal long	235